Near-field low-temperature photoluminescence spectroscopy of single V-shaped quantum wires

V. Emiliani and Ch. Lienau
Max-Born-Institut für Nichtlineare Optik und Kurzzeitspektroskopie, Rudower Chaussee 6, D-12489 Berlin, Germany

M. Hauert
University of Oxford, Clarendon Laboratory, Parks Road, Oxford OX1 3PU, United Kingdom

G. Colí, M. DeGiorgi, R. Rinaldi, A. Passaseo, and R. Cingolani
Unitá INFM, Department of Material Science, University of Lecce, I-73100 Lecce, Italy
(Received 15 October 1998; revised manuscript received 10 May 1999)

We report on a near-field spectroscopic study of single V-shaped $In_xGa_{1-x}As/GaAs$ quantum wires. With subwavelength resolution, the emission from single $In_xGa_{1-x}As$ wires and connecting planar quantum wells—separated by 250 nm—are individually resolved. The contributions of both monolayer height fluctuations on a 100 nm length scale and of short range compositional disorder to the localization of excitons in V-shaped quantum wires are separately identified and their implications for far-field PL spectra discussed. An upper limit for the migration length of the photogenerated excitons within the GaAs barrier layers of 250 nm is determined. [S0163-1829(99)01740-3]

During the last decade, quasi-one-dimensional (1D) semiconductor nanostructures—quantum wires—grown on patterned, V-shaped substrates (V-QWR) have attracted considerable interest,[1] partly due to their fundamental importance, and partly in view of their potential application in advanced optoelectronic devices. In particular, structures based on $In_xGa_{1-x}As$ are interesting candidates for applications in optical communications and model systems for studying the impact of the two-dimensional quantum confinement on the fundamental optical and electronic properties of 1D semiconductor nanostructures.[2–5]

Much of the information on the optical and electronic properties of V-QWRs has been obtained from photoluminescence studies. In such experiments, the distance between adjacent V-QWRs (typically between 0.5 and 1 μm) is generally smaller than the achieved spatial resolution, leading to the investigation of ensembles of up to 100 nanostructures. In order to reduce the pronounced inhomogeneous broadening in such ensembles and to elucidate the intrinsic 1D properties, experiments on single QWRs using microscopy techniques providing sub-micron spatial resolution are particularly desirable. A powerful candidate is near-field scanning optical microscopy[6,7] (NSOM) with resolution on the order of 100 nm. The potential of low-temperature near-field spectroscopy for the microscopic analysis of semiconductor nanostructures has been demonstrated in experiments on quantum wires fabricated by the cleaved edge overgrowth technique[8,9] and on patterned high-index (311)*A* GaAs surfaces,[10,11] in the latter structures also in combination with picosecond time-resolved techniques.[12]

In this paper, we report on a near-field photoluminescence study of V-groove quantum wires. Combining subwavelength spatial and spectral resolution, the emission from single $In_xGa_{1-x}As$ V-QWRs is spatially and spectrally resolved. Monolayer height fluctuations on a 100-nm length scale and short range compositional disorder are identified as the dominant disorder mechanisms that result in a spectral broadening of far-field PL spectra.

$In_xGa_{1-x}As/GaAs$ V-QWR samples were grown by subatmospheric pressure metal-organic chemical-vapor deposition (MOCVD) at 650 °C on a patterned (100), undoped GaAs substrate.[13] The patterned V-grooves exhibit a depth and periodicity of 250 and 500 nm, respectively. A nominally 3-nm-thick $In_{0.15}Ga_{0.85}As$ layer clad by thin GaAs layers was deposited into the grooves. Preferential nucleation results in a vertical $In_xGa_{1-x}As$ layer thickness of 9.5 nm at the bottom of the V groove.[13] The topmost GaAs cladding layer was etched down to about 60 nm to reduce the distance between V-QWR and sample surface to about 150 nm.

Far-field PL spectra at 10 K (Fig. 1) recorded with the excitation polarization perpendicular to the wire axis resolve clearly V-QWR emission at 1.413 eV and, around 1.44 eV, emission from the planar (100) QW region connecting adja-

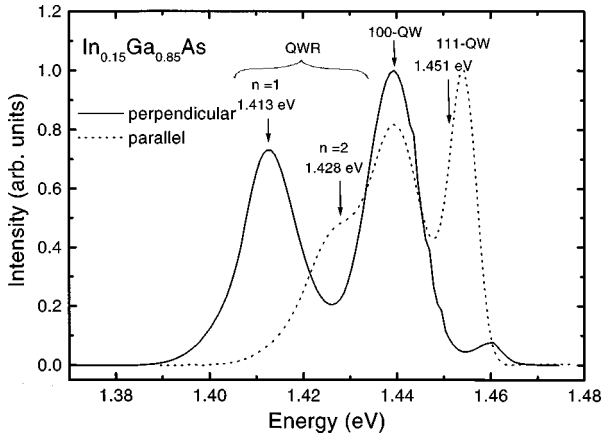

FIG. 1. Far-field PL spectra of the quantum wire sample at 10 K. The excitation is provided by an Ar^+ laser at 2.5 eV at an excitation density of 20 mW/cm^2. The continuous (dashed) lines were obtained with the polarization vector of the exciting beam perpendicular (parallel) to the quantum wire axis. The arrows indicate the calculated transition energies (see text).

cent grooves. The far-field spectra exhibit a strong polarization anisotropy, which is a signature of the one-dimensional character of the system. PL spectra for excitation parallel to the wire axis show strong emission from excited wire subbands together with (100) QW emission. In addition emission from the lateral QW region along the (111) groove sidewalls is observed around 1.455 eV. The peak assignment is in excellent agreement with calculations based on the solution of the two-dimensional Schroedinger equation of the system with inclusion of strain.

Near-field luminescence spectra are recorded at a sample temperature of 10 K in a home-built microscope.[14] Spatial resolution beyond the diffraction limit is obtained by transmitting excitation light from a HeNe laser through an aperture of about 150 nm at the end of a metal-coated fiber probe. The emitted photoluminescence (PL) is collected in the far-field, dispersed in a 0.22-m double monochromator with a spectral resolution of 0.8 meV and detected with a single-photon-counting silicon avalanche photodiode.

First V-QWR near-field photoluminescence spectra are shown in Fig. 2. Here, absorption of the HeNe excitation light creates electron-hole pairs in the near-field of the fiber aperture. The locally generated electron-hole pairs migrate through the nanostructure, on the time scale of the luminescence lifetime of about 500 ps,[3] until they get trapped in localized potential energy minima, e.g., within the $In_xGa_{1-x}As$ planar QW or the $In_xGa_{1-x}As$ V-QWR. The emission of these localized excitons is detected in the present experiment. Luminescence intensity is plotted as a function of detection energy (abscissa) and tip position (ordinate). The tip position was scanned in steps of 50 nm over a 2.0 μm range along a line perpendicular to the quantum wire axis, while the detection wavelength was scanned in 1 nm steps from 855 to 890 nm. The positions of the V-QWRs, separated by 500 nm, are depicted as dotted lines while those of the planar (100)-QW connecting adjacent grooves are shown as dashed lines.

In Fig. 2, emission occurring at the bottom of the grooves, containing the quantum wires, can both spectrally and spatially be distinguished from the emission originating at the planar parts of the structure connecting the wires. In particular, two spectral features are resolved in the planar (100)-QW region: (i) QW emission centered around 1.444 eV (859 nm), with a spectral width of 5–6 meV, and (ii) a weaker emission around 1.425 eV (870 nm) most likely related to a minor contribution of carbon impurities.

In the V-groove regions, V-QWR luminescence is emitted around 1.418 eV (874 nm). Intense emission from three wires is individually resolved and a splitting of the V-QWR emission spectrum of each of the three wires into (at least) two peaks separated by about 3 meV is found. In contrast to the QW emission, the peak positions of the wire emission are found to vary appreciably, by about 3 meV from wire to wire. Also the wire emission intensity fluctuates more strongly than that of the corresponding QWs.

The observation of both spatially and spectrally distinct emission bands from the planar QW and the V-QWR region gives direct information on the carrier exchange between these two regions. With the tip positioned at the center of each (100) QW mainly QW emission is detected. This shows that the photogenerated excitons are predominantly trapped into local energetic minima within the QW region and that exciton relaxation into low energy V-QWR states is inefficient. The thinning of the $In_xGa_{1-x}As$ layer along the sidewall separating V-QWR and QW that is observed in TEM images,[13] indicates that the carrier exchange between these regions is suppressed by local energetic barriers in the sidewall $In_xGa_{1-x}As$ layers.[10]

The occurrence of sharp doublets in the NSOM luminescence maps, separated by 3 meV, is reminiscent of radiative recombination of states localized at monolayer-high islands[15] formed at the bottom of the groove. Our calculations indicate that monolayer fluctuations at the bottom of the wire [along the (100) nanofacet] result in level splitting of the order of 1.7 meV per monolayer. The observed split lines thus suggest that the NSOM PL spectrum averages over two islands varying in thickness by 2 monolayers. Such islands have typical extensions of 100 nm and are randomly distributed along the wire profile, as observed by high-resolution atomic force microscopy at the bottom of the grooves.[16] Note that the split peaks in Fig. 2 that are assigned to monolayer fluctuations in individual wires are spatially separated by 50–100 nm. These separations are likely to reflect morphological imperfections at the bottom of the wires. The monolayer fluctuation lines have a width of about 5 meV, probably resulting from small random fluctuations of the composition of the wire material[15,17] (microroughness) on a length scale that is shorter than the typical island size and the exciton diameter.[18] Typical values for such a disorder-induced broadening amount to $\pm 0.3\%$, corresponding to 6–7 meV line broadening at low temperatures.

To study the effects of disorder along the wire axis, we recorded two-dimensional maps of the QW/V-QWR emission at fixed detection wavelengths (Fig. 3). The image shows four regions: (i) $0\ \mu m < y < 1.3\ \mu m$: here, the detection wavelength is set at 877 nm (V-QWR emission). (ii) $1.3\ \mu m < y < 2.55\ \mu m$: detection wavelength at 859 nm ($In_xGa_{1-x}As$ QW emission). (iii) $2.55\ \mu m < y < 3.9\ \mu m$: detection at 877 nm. (iv) $3.9\ \mu m < y < 5\ \mu m$: detection at 859 nm.

For detection at 877 nm, pronounced maxima of the V-QWR emission with a separation of about 500 nm, are observed. The location of these maxima is assigned to the center of the V grooves showing that the wire axis is oriented at about 18° with respect to the y axis. The intensity of the V-QWR emission is seen to fluctuate considerably between adjacent wires, the emission of few wires being reduced by more than 50%. The image shows pronounced fluctuations of the lateral wire-to-wire distance varying between 400 and 600 nm. Such fluctuations are indicative of a meandering of the groove distance, resulting from imperfections in the gratings. Typical observed length scales of fluctuations of the V-QWR emission intensity range from 100 to 1000 nm.

To analyze the spatial resolution we show in Fig. 4 sections taken across the x axis through Fig. 3. Figure 4(a) shows a clear modulation of the V-QWR emission intensity, with maxima that are separated by 485 nm. We define the modulation $M = 2*(I_{max} - I_{min})/(I_{max} + I_{min})$, with I_{max} being the emission intensity for excitation at the V-QWR location and I_{min} being that for excitation in the center between two wires. On average, the modulation M_{QWR} is 0.3, being very sensitive to the distance between adjacent grooves. The spa-

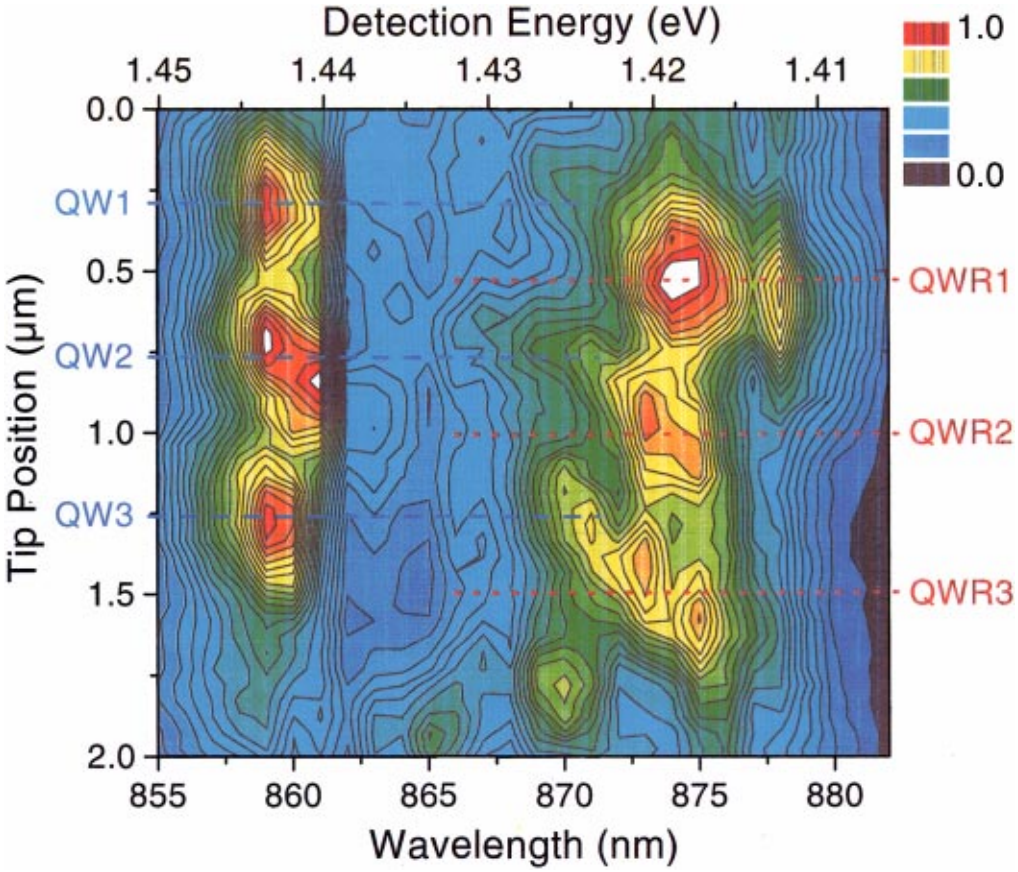

FIG. 2. (Color) Spatially resolved near-field photoluminescence spectrum at 10 K. The sample is excited by transmitting light from a HeNe laser through a 150-nm near-field aperture probe. Luminescence from the sample is collected as a function of tip position in the far field, spectrally dispersed and detected with a single photon counting photodiode. The positions of the V-QWRs are depicted as dotted lines, while those of the planar (100) QW connecting adjacent grooves are shown as dashed lines. Emission from the planar QW is centered around 1.443 eV and V-QWR emission around 1.418 eV.

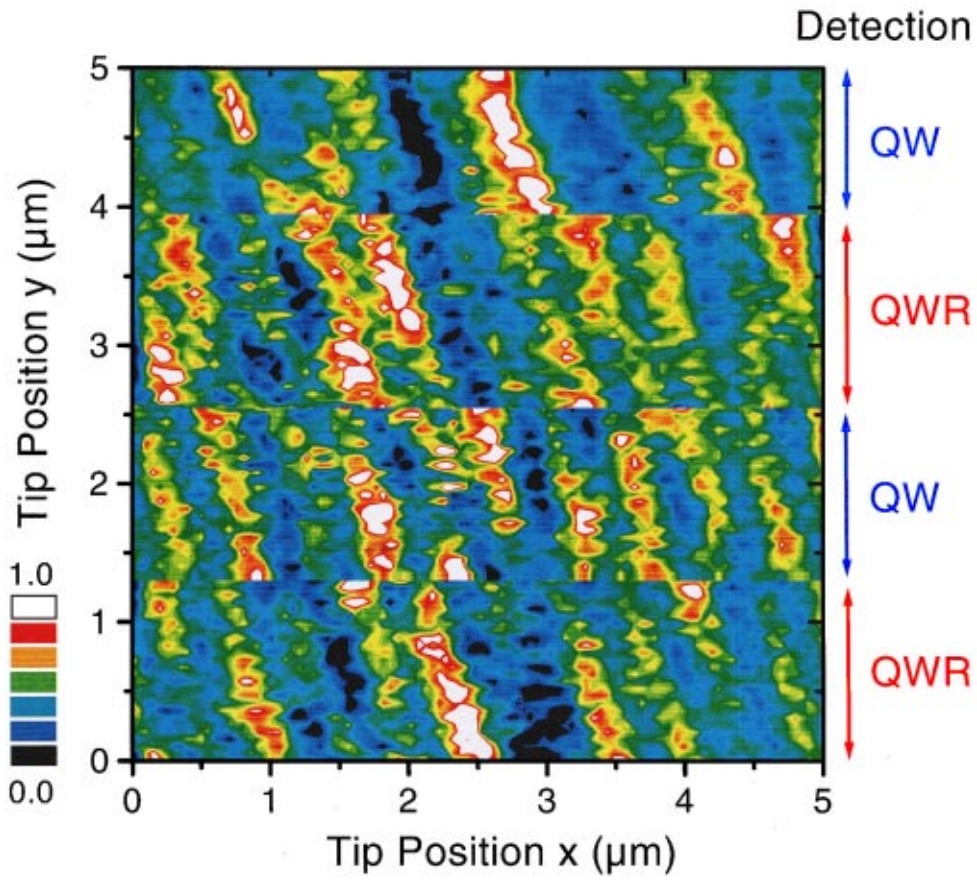

FIG. 3. (Color) Two-dimensional near-field luminescence image at a sample temperature of 10 K for detection at two fixed wavelengths, corresponding to the maximum of the QW and V-QWR emission, respectively. V-QWR luminescence at 877 nm is collected for $0\,\mu\text{m}<y<1.3\,\mu\text{m}$ and for $2.55\,\mu\text{m}<y<3.9\,\mu\text{m}$. Quantum well luminescence at 859 nm is collected for $1.3\,\mu\text{m}<y<2.55\,\mu\text{m}$ and for $3.9\,\mu\text{m}<y<5\,\mu\text{m}$. The wire axis is oriented at about 18° with respect to the y axis. Experimental conditions as in Fig. 2.

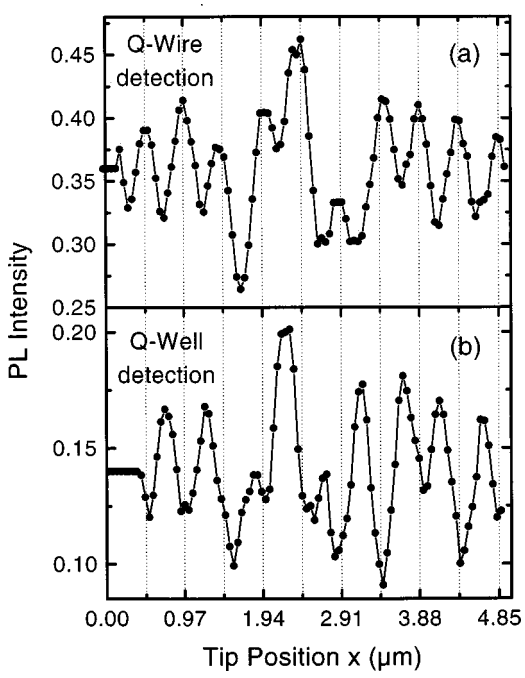

FIG. 4. Cross sections for (a) V-QWR detection and (b) QW detection.

tial variation of the V-QWR emission can reasonably be described by a sum of Gaussian profiles spatially separated with by 485 nm and with a full width at half maximum (FWHM) of 400 nm.

The signal detected at the (100)-QW emission, 859 nm, shows similar fluctuations as the V-QWR emission, both along the wire axis and between adjacent QWs [Fig. 4(b)]. The maxima are now located in the center between two V-QWR grooves, clearly demonstrating that QW and V-QWR emission are resulting from different regions of the sample. Moreover, the modulation of the QW emission M_{QW} is about two times larger than that of the V-QWR emission, on average $M_{\mathrm{QWR}}=2\times(0.18-0.10)/(0.28)=0.57$. This indicates a higher spatial resolution for QW detection than for V-QWR detection. We can describe the spatial variation of the luminescence profile again by a sum of spatially displaced Gaussians, now with a FWHM of 350 nm and offset by 250 nm compared to the profile in Fig. 4(a).

From the observed spatial resolution of 350 nm one can directly extract an upper limit for the exciton migration length within the GaAs barriers. Neglecting the width of the planar well, we estimate the spatial resolution of the QW PL scan as being given by a convolution of the limited spatial resolution of the electromagnetic near-field of about 250 nm and the diffusion-limited resolution due to exciton migration within the GaAs barriers. Assuming, for simplicity, Gaussian shapes for each of these profiles, the spatial resolution for QW detection can be estimated as $\mathrm{FWHM}_{\mathrm{QW}}=(L_d^2+d_{\mathrm{nf}}^2)^{1/2}$, with L_d being the exciton migration length, and d_{nf} the near-field resolution. With $\mathrm{FWHM}_{\mathrm{QW}}=350$ nm and $d_{\mathrm{nf}}=250$ nm, we find an upper limit for L_d of 250 nm. Considering the finite extension of the planar quantum well region of about 270-nm, that is another limiting factor for the resolution in this experiments, it is highly likely that the migration length of the excitons that give rise to QW luminescence is even smaller.

The decrease in spatial resolution for detection of V-QWR luminescence to 400 nm is related to the depth-dependent change in the lateral extension of the electromagnetic near-field. With increasing distance from the near-field aperture, the intensity of evanescent modes decays exponentially and the field distribution is dominated by the remaining propagating modes leading to a strong decrease in spatial resolution. In the investigated sample, the separation between V-QWR and surface of about 150 nm is substantial, explaining the loss of spatial resolution. Simplified models for the electromagnetic field distribution below nanosized apertures indicate that the lateral with of the near-field should correspond to about twice the value of the distance from the aperture. In our case, this would limit $d_{\mathrm{nf,QWR}}$ to about 300 nm and thus the overall resolution for detection of QWR luminescence $\mathrm{FWHM}_{\mathrm{QWR}}$ to about 390 nm, in good agreement with the experimental result.

In conclusion, we presented the first near-field spectroscopic study of individual V-shaped $In_xGa_{1-x}As/GaAs$ quantum wires. The dominant types of disorder leading to a spectral broadening of far-field PL spectra, namely monolayer height fluctuations of islands at the bottom of the V groove with a typical extension of 100 nm and small random fluctuations of the composition of the wire material on a length scale shorter than the exciton diameter, are directly identified. From the observed spatial resolution of the near-field images an upper limit of the exciton migration length within the GaAs barrier layers of 250 nm is determined, giving first information on the carrier transport processes in this complex nanostructure. Here, in particular studies combining the high spatial resolution of the near-field technique with (sub-) picosecond temporal resolution shall be of great value for increasing this knowledge.

One of the authors (V.E.) is grateful to the Alexander von Humboldt Foundation for assistance and financial support. M.H. thanks the European Union for support.

[1] E. Kapon *et al.*, Phys. Rev. Lett. **63**, 430 (1989).
[2] R. Rinaldi *et al.*, Phys. Rev. Lett. **73**, 2899 (1994).
[3] M. Lomascolo *et al.*, J. Appl. Phys. **83**, 302 (1998).
[4] R. Ambigapathy *et al.*, Phys. Rev. Lett. **78**, 3579 (1997).
[5] F. Vouilloz *et al.*, Phys. Rev. Lett. **78**, 1580 (1997).
[6] D. W. Pohl, W. Denk, and M. Lanz, Appl. Phys. Lett. **44**, 651 (1984).
[7] E. Betzig and J. K. Trautman, Science **257**, 189 (1992).
[8] R. D. Grober *et al.*, Appl. Phys. Lett. **64**, 1421 (1994).
[9] T. D. Harris *et al.*, Appl. Phys. Lett. **68**, 988 (1996).
[10] A. Richter *et al.*, Phys. Rev. Lett. **79**, 2145 (1997).
[11] Ch. Lienau *et al.*, Phys. Rev. B **58**, 2045 (1998).
[12] A. Richter *et al.*, Appl. Phys. Lett. **73**, 2176 (1998).
[13] A. Passaseo *et al.*, J. Cryst. Growth **197**, 777 (1999).
[14] G. Behme *et al.*, Rev. Sci. Instrum. **68**, 3458 (1997).
[15] D. Gammon *et al.*, Phys. Rev. Lett. **76**, 3005 (1996).
[16] R. Cingolani *et al.*, Phys. Rev. B **58**, 1962 (1998).
[17] M. Ramsteiner *et al.*, Phys. Rev. B **55**, 5239 (1997).
[18] C. A. Warwick and R. F. Kopf, Appl. Phys. Lett. **60**, 386 (1996).